



Kent Academic Repository

Barker, Robert (2019) *Block CopolymersBased Nanoporous Thin Films with Tailored Morphology for Biomolecules Adsorption*. *Advanced Materials Interfaces*, 7 (5). ISSN 2196-7350.

Downloaded from

<https://kar.kent.ac.uk/79054/> The University of Kent's Academic Repository KAR

The version of record is available from

<https://doi.org/10.1002/admi.201901580>

This document version

Author's Accepted Manuscript

DOI for this version

Licence for this version

CC BY-NC-ND (Attribution-NonCommercial-NoDerivatives)

Additional information

Versions of research works

Versions of Record

If this version is the version of record, it is the same as the published version available on the publisher's web site. Cite as the published version.

Author Accepted Manuscripts

If this document is identified as the Author Accepted Manuscript it is the version after peer review but before type setting, copy editing or publisher branding. Cite as Surname, Initial. (Year) 'Title of article'. To be published in *Title of Journal*, Volume and issue numbers [peer-reviewed accepted version]. Available at: DOI or URL (Accessed: date).

Enquiries

If you have questions about this document contact ResearchSupport@kent.ac.uk. Please include the URL of the record in KAR. If you believe that your, or a third party's rights have been compromised through this document please see our [Take Down policy](https://www.kent.ac.uk/guides/kar-the-kent-academic-repository#policies) (available from <https://www.kent.ac.uk/guides/kar-the-kent-academic-repository#policies>).

Block Copolymers-based Nanoporous Thin Films with Tailored Morphology for Biomolecules Adsorption

Anna Malafronte^{§}, Finizia Auriemma^{*§}, Chiara Santillo[§], Claudio De Rosa[§], Rocco Di
Girolamo[§], Robert Barker^{‡†}, Yuri Gerelli[‡]*

[§]Dipartimento di Scienze Chimiche, Università di Napoli Federico II, Complesso Monte S.
Angelo, Via Cintia, 80126 Napoli, Italy

[‡] Institut Laue-Langevin, 71 Avenue des Martyrs, 38000 Grenoble, France.

KEYWORDS: block copolymers, self-assembly, nanostructures, nanoporous surfaces,
biomolecules adsorption.

ABSTRACT

We report the fabrication of nanoporous thin films based on di-block copolymers (BCPs) able to act as ideal support for the physical immobilization of specific biomolecules. The nanoporous thin films, fabricated by exploiting self-assembly of lamellar BCPs and the concept of sacrificial block, are characterized by a well-defined architecture and morphology containing functionalized pores delimited by hydrophilic walls. In particular, the material exhibits a lamellar morphology with nanochannels of width ≈ 20 nm delimited by polystyrene (PS) domains, decorated with pendant poly(ethylene oxide) (PEO) chains. We perform an in depth analysis of the adsorption of myoglobin (Mb) onto our BCP-based nanoporous material by means of UV-Visible spectroscopy, quartz crystal microbalance (QCM) and neutron reflectometry (NR) measurements, comparing the results with those obtained in the case of supports having different hydrophilicity, chemical composition and morphology (e.g. non-porous PS thin films and nude glass slides). The adsorption capability of the BCP-nanoporous surface results remarkably higher than of both flat and hydrophilic (glass slides) and flat and hydrophobic surfaces (PS) due to the large surface area and opened pore structure that allows high protein loadings. Remarkably, quite strong interactions are established between the biomolecules and our porous surface by effect of simple physical adsorption.

Introduction

Understanding proteins adsorption process from an aqueous environment to a solid surface is a major concern in a number of fields such as biology, biotechnology, biochemical engineering, biomedicine, environmental science and industrial catalysis.¹⁻⁷ The adsorption of proteins at solid/liquid interfaces is not only a fundamental phenomenon³ but it is also the key to several practical applications, since in many cases adsorption behavior and interaction between proteins and sorbent surfaces play an important role in determining the performance of a designed system, such as biosensors,^{4,5} immunological tests and drug-delivery schemes.⁶ The immobilization of the biorecognition element to the surface of a solid support is, for example, a critical step for the development of efficient biosensors,^{4,5} since immobilization of the biomolecule to various inorganic, organic or polymeric matrices by simple adsorption, covalent bonding or entrapment improves enzyme stability, increases its rigidity and, consequently, prevents the possibility to unfold and deactivate, this being one of the main drawbacks that impeded biosensors large-scale application as reliable analytical instruments. The quantitative characterization of how surface features determine the amount, structure and distribution of adsorbed proteins is also important in biomaterial field, since surfaces in biological environments are rapidly coated by proteins that mediate the interaction between the material and cells, regulating the final cell behavior through complex signaling pathways.⁸

Surface nanoscale morphology has a relevant role in regulating the interaction between support and biomolecules and profoundly influences the process of biomolecules adsorption.⁹⁻¹³ This concept has sparked new research approaches, where the control of surface nanostructure is used as a material design parameter to regulate adsorption of proteins for specific applications. The knowledge of the protein adsorption process on nanostructured surfaces is relevant to many

research fields such as tissue regeneration,¹⁴ drug delivery,¹⁵ prosthetics,¹⁶ nanotoxicology,¹⁷ biosensing,^{18,19} and therapeutic micro- and nano-devices.²⁰ Several attempts have been made to characterize the influence of nanoscale morphology on protein adsorption and experiments specifically designed to characterize protein adsorption on nanostructured surfaces resulted in quite inconsistent observations. Some reports showed no influence of the morphology at the nanoscale level,^{10,11} while others presented an increase of the amount of adsorbed proteins when nanoscale surface roughness increased.^{12,13} This incoherent picture arises from the fact that protein adsorption on nanostructured surfaces has never been fully quantitatively characterized, both because of the remarkably large number of parameters affecting the adsorption process, and because of the lack of suitable tools for studying adsorption on rough surfaces. A full characterization of protein adsorption onto a nanostructured surface should consist of a controlled variation of the following parameters: nanoscale morphology, protein concentration and protein type. Varying surface morphology requires, in particular, the fabrication of nanostructured surfaces with exactly controllable domain size, chemical composition and surface roughness, in order to draw definitive conclusions. In addition, the presence of controlled nanoporosity onto the surface has to be considered, since the large surface area of nanoporous materials and their opened pore structure can be beneficial for the process of adsorption of biomolecules. Nanoporosity can afford improved enzyme loading, which in turn can increase the apparent enzyme activity per unit mass or volume, compared with that of enzymes immobilized onto conventional non-porous materials.²¹⁻²³

We previously reported²³ the fabrication of a nanoporous material based on di-block copolymers (BCPs), with well-defined architecture and morphology, containing functionalized pores delimited by hydrophilic walls, able to act as ideal support for the physical immobilization

of specific biomolecules. In particular, nanoporous thin films were fabricated by exploiting self-assembly of lamellar BCPs and the concept of sacrificial block.

A BCP molecule can self-assemble to form nanostructures (having lamellar, hexagonally packed cylindrical, bicontinuous gyroid, or body centered cubic (BCC) spherical morphology) with a domain spacing (typically in the range 10-200 nm) that depends on molecular mass, segment size, and the strength of interaction between the blocks.²⁴⁻²⁶ Nanoporous materials can be generated by selective removal of one block from a self-assembled BCP by using selective etching protocols that do not compromise the integrity of the matrix material.²⁷⁻³⁰ The etching protocols creates nanopores in the final material, that will exhibit the pore size and pore topology of their parent structures.

We employed a blend of polystyrene-*block*-poly(L-lactide) (PS-PLLA) and polystyrene-*block*-poly(ethylene oxide) (PS-PEO) di-block copolymers to generate thin films with a lamellar morphology in which the PEO and PLLA blocks form mixed lamellar domains alternating with PS domains (Figure 1a). Then, by selective chemical etching of the PLLA blocks, nanoporous thin films, patterned with nanometric channels containing pendant hydrophilic PEO chains, were generated (Figure 1b). We previously demonstrated²³ that the large surface area, the tailored pore sizes, and the functionalization with hydrophilic PEO blocks, make the designed nanostructured materials suitable supports for the nanoconfinement of the enzyme Peroxidase from Horseradish (HRP). The use of our porous films as confining support for the HRP improved the catalytic performance of the enzyme without mass-transfer limitations and the presence of pores makes the long-term stability of immobilized enzyme high.

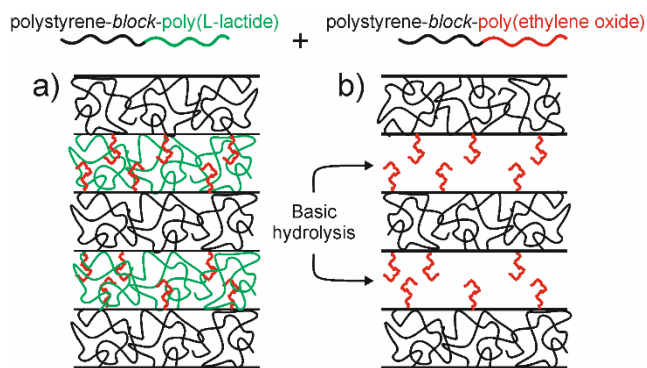


Figure 1. Step strategy used to obtain the BCP-based nanoporous material. (a) The starting material is a nanostructured thin film in lamellar morphology, obtained by mixing polystyrene-*block*-poly(L-lactide) (PS-PLLA) and polystyrene-*block*-poly(ethylene oxide) (PS-PEO) block copolymers. PS lamellar domains alternate with PLLA block domains mixed with PEO blocks; (b) Selective removal of PLLA by basic hydrolysis leaves nanometric channels delimited by PS domains grafted with pendant PEO chains. Adapted from Ref. 23.

In this study, the strength of our approach is probed by performing an in depth analysis of the adsorption of myoglobin (Mb) onto our BCP-based nanoporous material (Figure 1b) by means of UV-Visible spectroscopy, quartz crystal microbalance (QCM) and neutron reflectometry (NR) measurements. In particular, the adsorption capability of Mb onto our nanoporous surfaces is studied and compared with that obtained in the case of supports having different hydrophilicity, chemical composition and morphology (e.g. non-porous polystyrene (PS) thin films and nude glass slides). The aim of this study is to compare the Mb adsorption onto the different supports and to identify the key parameters determining the mutual affinity of the biomolecule with the support including the role of nanopores.

Experimental Section

Preparation and characterization of PS thin films and BCP-based materials.

The main characteristics of the PS and BCP samples are described in the Supporting Information. The volume fraction of the PS block in the BCPs was selected equal to ≈ 0.50 to obtain a lamellar phase-separated morphology. Solutions at 0.5% or 1% w/w concentration of the sole PS or of PS-PLLA and PS-PEO blends at 90/10 w/w ratio were prepared by dissolving the polymers in 1,2-dichloroethane. Thin films were obtained by spin coating (RPM 3000 for 30 s) the solutions onto silicon, gold or glass supports. The lamellar morphology of the BCPs thin films was improved by heating the samples to 200 °C and then cooling to room temperature on a hot bench with a gradient temperature. Nanoporous supports were obtained by removing the PLLA blocks from the nanostructured BCPs thin films through basic hydrolysis, performed by placing the thin films of the blend into a 0.5 M sodium hydroxide water/methanol (60:40 by volume) solution at 65°C for one minute (etching procedure). The films were then withdrawn from the solution, washed twice with a water/methanol (60:40 by volume) solution, and finally dried in a hood at room temperature overnight. For UV-Vis spectroscopy experiments, thin films of PS and etched blend were prepared onto glass supports (size 24x24 mm). For NR measurements, the samples were prepared onto crystalline and polished silicon (111) wafers (size 80x50x10 mm) that bear a thin amorphous silicon oxide (SiO₂) layer at the surface. For QCM measurements, the samples were directly prepared onto the gold working electrode of the AT-cut crystal of the microbalance. We checked that the supports were uniformly covered by the polymer (PS) and BCP-based thin films, taking electron microscopy images of different quadrants of the specimens in regions both close to the boundaries and in the center.

Experiments of myoglobin adsorption.

UV-Vis spectroscopy. The adsorption kinetics of myoglobin (Mb) onto different supports were probed through UV-Vis spectroscopy using a Cary 60 UV-Vis spectrophotometer equipped with a Cary single cell Peltier accessory (Agilent Technologies). Solutions of Mb at different concentrations were prepared in distilled water. Adsorption of Mb onto different supports was measured in isothermal conditions by deposition of solutions onto supports, at constant Mb concentration, as a function of incubation time to obtain adsorption kinetics curves, and at constant incubation time, as a function of Mb concentration to obtain adsorption isotherm curves. In particular, measurements of adsorption kinetics were performed at 5 °C by depositing 750 µL of solutions at Mb concentrations of 3.75, 4.03, 6.39 and 7.95 mg/L onto our nanoporous film surface, as a function of the incubation time (ranging from 5 to 75 minutes). For comparison, these experiments were also conducted using PS thin films as support, in the case of solutions at Mb concentration of 4.03 and 7.95 mg/L. The measurements of adsorption isotherms were performed at 5 and 10 °C by depositing 500 µL of solutions at Mb concentrations of 2.22, 3.44, 5.35 and 8.62 mg/L onto different supports (nanoporous film surface, PS thin films or nude glass slides), fixing the incubation time to 30 min. During the incubation the samples were placed onto an oscillating stirrer. After any selected incubation time, the supernatant protein solution was withdrawn from the films surface and the samples were rinsed with distilled water to remove weakly adsorbed protein molecules from the surface. UV-Vis spectroscopy and High Performance Liquid Chromatography (HPLC, **DECLINARE LE SPECIFICHE DELL'APPARATO tra parentesi**) indicated that no detectable amount of protein was present in the rinsing water, already in the first cleaning wash. The myoglobin concentrations of the initial solution and of the recovered solution were both determined by UV-Vis adsorption

measurements using the absorbance of the band at 408 nm (molar extinction coefficient value of $188000 \text{ M}^{-1} \text{ cm}^{-1}$).^{31,32} The amount of adsorbed myoglobin onto the supports $\Gamma(t)$, after the incubation time t and normalization for the adsorbing area A , was estimated from the difference in the myoglobin concentration in the recovered solutions $C_r(t)$ and in the solutions initially deposited on the supports C_0 , according to Equation 1;

$$\Gamma(t) = \frac{V_0(C_0 - C_r(t))}{A} \quad (\text{Eq. 1})$$

In Equation 1 the adsorbed amount of protein per unit surface area or surface density coverage $\Gamma(t)$, is function not only of the incubation time t but also of the concentration of the solutions initially deposited on the supports C_0 . Moreover, V_0 is the volume of the initial protein solution and A , the surface area of the support, is equal to $576 \text{ mm}^2 (= 24^2 \text{ mm}^2)$.

All experiments were performed in triplicate achieving a high reproducibility.

The data of Mb adsorption were analyzed by using the Langmuir equation:

$$\frac{\Gamma(t)}{\Gamma_m} = \frac{KC_0}{1 + KC_0} \quad (\text{Eq. 2})$$

that can be transformed into the linear form:

$$\frac{C(t)}{\Gamma(t)} = \frac{1}{K\Gamma_m} + \frac{C(t)}{\Gamma_m} \quad (\text{Eq. 3})$$

In Equation 3 Γ_m is the maximum value of protein surface density coverage (full coverage of surface, or monolayer adsorption density) and indicates the monolayer adsorption ability on the surface, and K is the adsorption-to-desorption ratio, or Langmuir binding constant for the adsorption process.

QCM measurements. A QCM apparatus (Novaetech S.r.l.) equipped with a disc-shaped, AT-cut piezoelectric quartz crystal (fundamental resonant frequency 10 MHz), having metal gold

electrodes with diameter 4.5 mm deposited on its two faces, was used. A mass deposition onto the electrode induces an increase in frequency which is proportional to the adsorbed mass. In particular, for the quartz crystals used in this study, a frequency change of 1 Hz corresponds to a mass increase of 0.70 ng, and to a sensitivity of 1.43 Hz ng⁻¹. Nanoporous BCP-based thin films were directly prepared onto the gold electrode of the crystal, according to the procedure described above. The resonance frequency of the crystal was measured at 25 °C after coating with the blend thin film in a first step, the nano-porous thin film in a second step and after a third step involving Mb adsorption onto the so-coated electrode. In particular, this third step was performed at 5 °C by depositing 40 µL of Mb solutions (concentration 6.6 mg/L) onto the Au electrode functionalized with the nano-porous material, using the same protocol explained before. Measurements were performed after an incubation time of 5, 20 and 50 min, successive washing with water to remove loosely bound proteins, and drying process at room temperature overnight to remove water excess.

Neutron reflectometry (NR). NR measurements were performed on the D17 reflectometer at the Institut Laue-Langevin (Grenoble, France).^{33, 34} The sample cell consisted of a PTFE reservoir containing water solutions put against a silicon supports sandwiched between two aluminum plates used for thermal control. The sample cells were kept at a temperature of (25.0 ± 0.5) °C during the experiments. The specular reflectivity signal, R , defined as the ratio of the number of reflected neutrons with respect to that of incident ones, was measured at an angle equal to the angle of incidence, θ_i , and as a function of the component of momentum transfer vector Q in the perpendicular direction to the sample surface $Q_z = \sin(\theta_i) 4\pi/\lambda$, where λ is the neutron wavelength. Measurements were carried out in time-of-flight (ToF) mode with a wavelength range 0.2 - 2 nm at two fixed angles of incidence, $\theta_i = 0.8^\circ$ and $\theta_i = 3.2^\circ$, to cover a range of Q_z

ranging between 0.08 and $\sim 2 \text{ nm}^{-1}$ (the upper limit being defined by the experimental background). The Q_z -dependence of reflectivity depends on the nuclear composition of the sample in the Z-direction. This information is commonly expressed in terms of neutron scattering length density profile (SLD).^{35, 36} It is important to note that an SLD profile usually represents the average in-plane (parallel to the interface) SLD value as a function of the z -coordinate. In the case of in-plane patterned films, where the lateral separation between regions of the sample with different scattering properties is larger than the lateral coherence length of the incident neutrons, reflectivity can be interpreted as the sum of the individual reflectivity originated by the different in-plane regions. This method is known as incoherent sum. We first characterized by NR silicon supports coated with thin films of PS and PS-PLLA/PS-PEO blend before and after removal of PLLA, in three different contrast liquids (See Supporting Information, Part S1, for further experimental details), and then NR characterization was extended to the coated silicon supports after protein adsorption. A D₂O solution of myoglobin at a concentration of 0.45 μM (7.9 mg/L) was used for incubation, imposing an incubation time (equilibration) of 3 h before NR measurements. In the case of the etched blend, the protein solution was removed by rinsing 3 times with 10 mL of H₂O, and the reflectivity profiles were measured again in presence of D₂O.

Results and discussion

A representative Field Emission Scanning electron microscopy (FESEM) image of thin films of the polystyrene-*block*-poly(L-lactide) (PS-PLLA) and polystyrene-*block*-poly(ethylene oxide) (PS-PEO) blend (at 90/10 w/w ratio) is reported in Figure 2A. A well-defined phase separated morphology, characterized by a disordered array of lamellar domains oriented perpendicular to the support, is visible. The bright lamellar domains correspond to PS lamellar nanodomains and the dark regions correspond to mixed PEO and PLLA component, as in the scheme of Figure 1a.

The average lamellar spacing of PS and PEO/PLLA domains is estimated to be $\approx 28 \pm 5$ and $\approx 20 \pm 5$ nm, respectively.

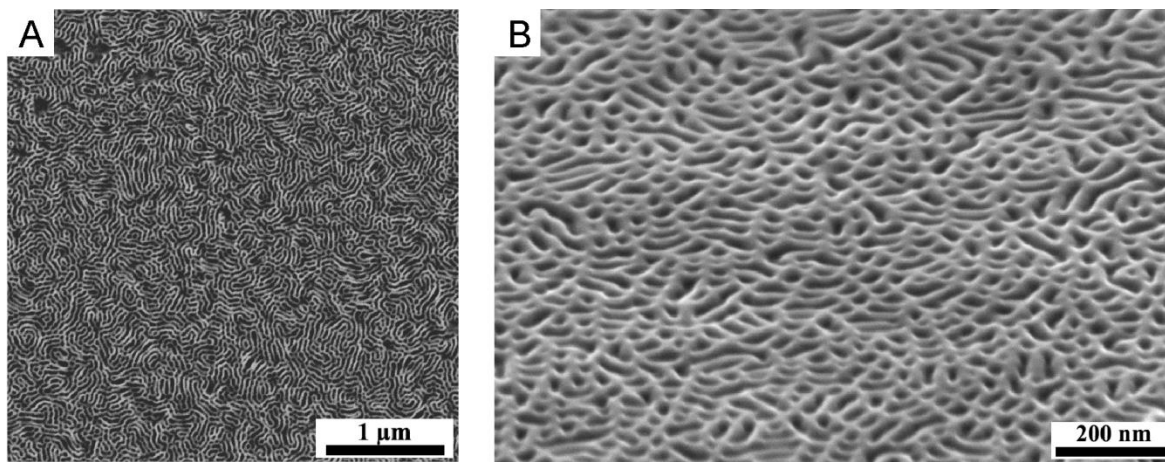


Figure 2. FESEM images of a thin film of the blend PS-PLLA/PS-PEO blend before (A) and after (B) removal of PLLA. Tilt angle of the image in B is 66.2° . The typical thickness of the films is 40-100 nm.

A FESEM image of the thin film of the blend after removal of PLLA blocks by basic hydrolysis is reported in Figure 2B. The etching treatment does not alter the initial lamellar morphology and results in porous thin films with nanochannels of width ≈ 20 nm delimited by PS lamellar domains, decorated with pendant PEO chains, as in the scheme of Figure 1b. A full characterization of the BCP-based nanoporous material is reported in [Ref. 23](#).

We studied the adsorption kinetics of myoglobin (Mb) onto our BCP-based nanoporous supports (Figures 1b and 2B) by deposition of protein solutions onto the supports as a function of the contact time between the protein solutions and the supports (incubation time). In particular, measurements were performed at incubation times ranging from 5 to 75 min, at fixed Mb concentrations in between 3.75 and 7.95 mg/L. Equation 1 was used to determine the adsorbed amount of protein per unit surface area (surface density coverage) ($\Gamma(t)$) as a function of

incubation time. We verified that the BCP-based nanoporous materials retained the morphology after the contact with aqueous solutions containing Mb even for the longest incubation time (75 min, Figure S1). The kinetics of Mb adsorption onto our nanoporous supports (Figures 1b and 2B) are reported in Figure 3A. Two kinetic regimes are identified depending on the initial concentration of Mb in the solutions used for incubation, corresponding to a low concentration regime, for Mb concentration less than ≈ 4 mg/L (curve a of Figure 3A), and a high concentration regime, for Mb concentration higher than ≈ 6 mg/L (curve b of Figure 3A). In both cases the surface density coverage ($\Gamma(t)$) increases steeply in the first 5-10 min of incubation, up to reach values $\Gamma(30)$ of ≈ 2 and ≈ 3 ng/mm² at low and high Mb concentration after 30 min incubation time, respectively. Considering that the molecular mass of Mb is 17.6 Kg/mol, the values of surface density coverage of 2 or 3 ng/mm² correspond to adsorption of ≈ 1 molecule of Mb each 10 nm². A footprint area of 10 nm² per Mb chain is in agreement with the side area of this disk-like protein estimated from crystal structure analysis of 4.4 nm x 4.4 nm x 2.5 nm.^{37,38} In particular, the observed change in the adsorption capability of the nanoporous surface with the concentration of Mb in the solution used for incubation may reflect changes in the orientation of the binding protein, eventually leading to changes in protein-surface interactions at the interface.

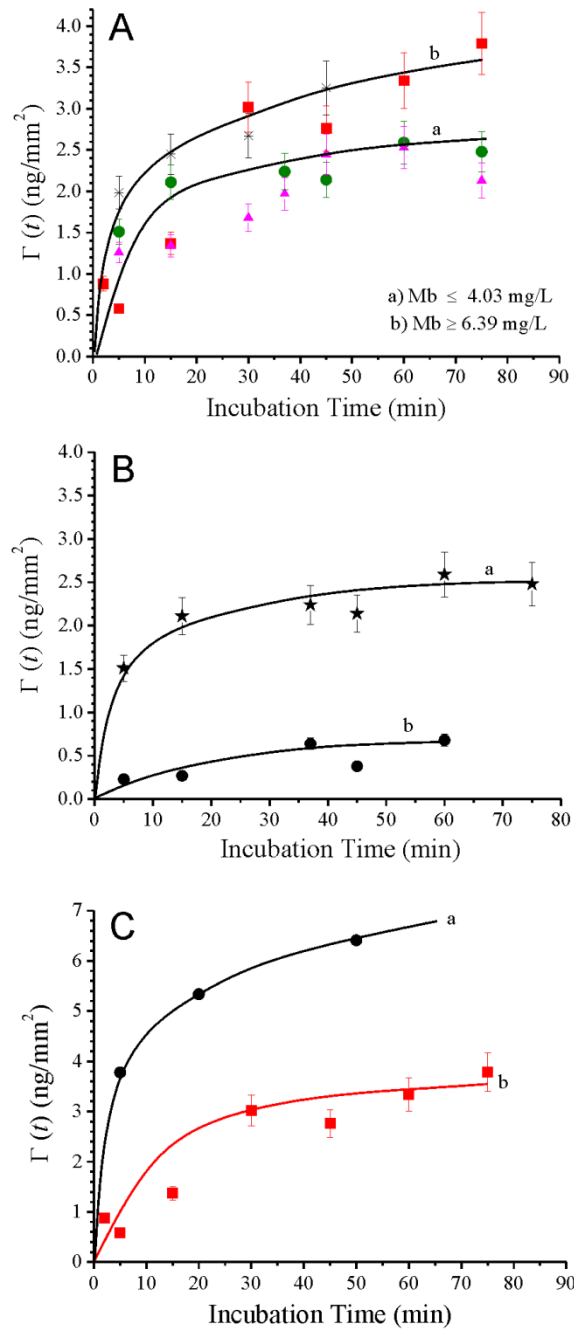


Figure 3. (A) Adsorption kinetics of myoglobin (Mb) onto the BCP-based nanoporous supports measured at 5°C. The surface density coverage of Mb ($\Gamma(t)$) was determined using Equation 1 after different incubation times (ranging from 5 to 75 min) fixing the concentrations of the initial solutions of Mb to 3.75 (▲), 4.03 (●), 6.39 (■) and 7.95 (✱) mg/L. (B) Comparison between the

kinetics of Mb adsorption at 5°C onto the BCP-based nanoporous material (curve a) and PS thin film (curve b) fixing the concentration of the initial Mb solution to 4.03 mg/L. (C) Comparison between the data of Mb adsorption kinetics at 5°C onto the nanoporous material obtained from QCM (curve a) and UV-Vis (curve b) measurements fixing the concentration of the initial Mb solution to 6.6 mg/L (a) and 6.39 mg/L (b).

The Mb adsorption kinetics onto our nanoporous surface are compared with those onto PS in Figures 3B and S2, using initial Mb concentrations of 4.03 (Figure 3B) and 7.95 (Figure S2) mg/L. It is evident that the mass of protein absorbed onto the nano-porous surface of the etched blends is ≈ 4 and ≈ 2 times higher than that absorbed onto PS, using a Mb concentration in the initial solution of ≈ 4 (Figure 3B) and ≈ 8 (Figure S2) mg/L, respectively. Therefore, the adsorption capability of the BCP-nanoporous surface is remarkably higher than that of PS.

We also studied the kinetics of Mb adsorption by mean of quartz crystal microbalance (QCM) measurements. To this aim the gold working electrode of the AT-cut crystal of the QCM was coated with our nano-porous thin films, using the procedure described in the Experimental Section. We verified that the morphology of the BCP thin film was retained onto the gold surface (Figure S3). Mb was physically adsorbed onto the same electrode by placing solutions of Mb with a fixed concentration (6.6 mg/L) onto the porous material for different incubation times (5, 20 and 50 min) at 5 °C. Then, after removal of the Mb solutions, the crystal was washed with water, to remove loosely bound protein chains, and dried at room temperature overnight. The mass of absorbed Mb was determined by measuring the resonance frequency of the coated electrode before (corresponding to mass M_C) and after (corresponding to mass M_{CP}) Mb adsorption, as the difference $M_{CP} - M_C$. QCM frequency vs. time graphs obtained during the

consecutive steps of the procedure to prepare the BCP-based nanoporous material onto the QCM crystal and the subsequent Mb adsorption onto the so-coated crystal, in the case of a Mb incubation time equal to 20 min, is reported in Figure S4.

A comparison between the kinetics of Mb adsorption onto the BCP-based porous material obtained by using QCM and UV-visible technique is reported in Figure 3C (curves a and b, respectively). As expected, QCM senses a much higher mass uptake in comparison with the optical techniques (compare curves a and b of Figure 3C). In particular, for incubation times longer than 30 minutes, the mass of adsorbed protein measured with QCM is higher by a factor of ≈ 2 than the mass measured with the optical technique, in agreement with the results obtained in a large number of other studies for small and globular proteins.³⁹⁻⁴¹ The general observation that the values of mass uptake of a protein from a given support as determined by QCM are remarkably higher than those determined by optical spectroscopy can be attributed to presence of water molecules which are tightly bound and/or hydrodynamically trapped to the adsorbed proteins.

Isothermal adsorption experiments of Mb was also performed at 10 °C onto our nanoporous support (etched blend), non-porous thin films of PS and glass surfaces, using a fixed incubation time of 30 min. The results are reported in Figure 4, and in Table 1. It is apparent that after 30 min incubation time the $\Gamma(30)$ values in the case of our nanoporous surface (curves a, a' of Figure 4) is higher than that of both the PS thin film (curve b of Figure 4) and the glass slide (curve c of Figure 4), regardless of the Mb initial concentrations (C), whereas the amount of adsorbed Mb on the PS thin film and the glass slide are similar (curves b and c of Figure 4).

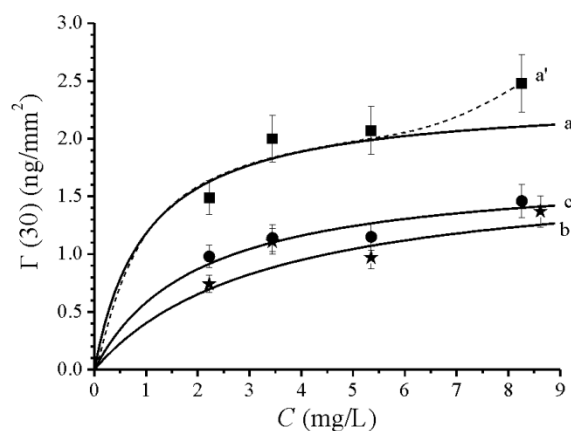


Figure 4. Adsorption isotherms of myoglobin onto thin films of the etched nanoporous blend (a, a', ■), PS (b, ★) and bare glass slides (c, ●). Incubation was performed for 30 min, at 10 °C. The solid lines a, b and c are the fit to the data with the Langmuir equation (Equation 2). The dashed line a' shows the deviation from the Langmuir fit in the case of the etched blend.

We found that the amount of adsorbed protein increases with increasing the protein concentration in the initial solutions, according with the existence of the concentration dependent process named “spreading”, that is, the increment of the footprint of the protein with the residence time of the protein onto the sorbent.⁴² At higher concentrations of the initial solution, the biomolecules occupy the surface in a shorter time and the time for spreading is small. As a consequence, the footprint of the proteins is small and an higher amount of protein can be adsorbed. All isotherms of Figure 4 were fitted to the Langmuir isotherm equation. The monolayer adsorption density (Γ_m) and Langmuir binding constant (K) values obtained by plotting C/Γ vs C (Equation 3, Figure 5A) are reported in Table 1.

Table 1 Surface density coverage ($\Gamma(30)$) and number of myoglobin biomolecules adsorbed per nm^2 (n_{Mb}) onto the BCP-based nanoporous material (etched blend), PS thin film and bare glass slide for different initial concentrations of the protein in the solutions (C), after an incubation time of 30 min at 10°C . Monolayer adsorption density (Γ_m) and Langmuir binding constant (K) calculated by fitting the adsorption isotherms of Figure 4 with linearized form of Langmuir equation (Equation 3).

	$\Gamma(30)$ (ng/mm^2) ^(a)				Γ_m (ng/mm^2) ^(b)	n_{Mb} (units/nm^2) ^(c)	K ^(b)
	C 2.22 (mg/L)	C 3.44 (mg/L)	C 5.35 (mg/L)	C 8.62 (mg/L)			
Etched Blend	1.5 ± 0.1	2.0 ± 0.2	2.1 ± 0.2	2.5 ± 0.2	2.7 ± 0.2	$(9.2 \pm 0.7) 10^{-2}$	1.0 ± 0.5
PS	0.7 ± 0.1	1.1 ± 0.1	1.0 ± 0.1	1.4 ± 0.1	1.7 ± 0.5	$(5.8 \pm 0.2) 10^{-2}$	0.3 ± 0.2
Glass slide	1.0 ± 0.1	1.1 ± 0.1	1.1 ± 0.1	1.4 ± 0.1	1.7 ± 0.2	$(5.8 \pm 0.1) 10^{-2}$	0.5 ± 0.2

a) Maximum relative errors calculated considering an error of 10% in the volumes of the retrieved Mb solutions.

b) Absolute errors calculated by propagation of the maximum error. Results are averaged over at least three independent experiments.

c) Number of protein molecules per nm^2 calculated as: $\Gamma_m 10^{-21} \text{NA} / 17600$, where 17600 g/mol is the molecular mass of myoglobin and NA is the Avogadro number.

From the calculated values of Γ_m and K (Table 1) it is evident that our porous BCP film is a better support for Mb adsorption than the PS thin film and the glass slide. In particular, the fit of adsorption data onto the nanoporous surface of the BCP blends gives a value of the Langmuir binding constant for the adsorption process $K=1$ and a maximum value of the protein surface density coverage of $2.7 \text{ ng}/\text{mm}^2$, which are higher than those fitting the adsorption data in the case of PS and glass slides (Table 1). The apparent number of myoglobin biomolecules adsorbed per nm^2 (n_{Mb} , see Table 1) calculated from the Γ_m value is $n_{\text{Mb}} \approx 9 \times 10^{-2} \text{ units}/\text{nm}^2$ in the case of the nanoporous support (etched blend) and $n_{\text{Mb}} \approx 6 \times 10^{-2} \text{ units}/\text{nm}^2$ in the case of non-porous supports (PS and glass), corresponding to a single Mb biomolecule adsorbed on an area A of $\approx 11 \text{ nm}^2$ in the case of the porous support and $\approx 17 \text{ nm}^2$ in the case of the non-porous supports.

This is due to the large surface area and opened pore structure that allows high protein loadings in the case of the etched blend. The results that our support exhibits an increased adsorption ability with respect to both a flat and hydrophilic surface (glass slide) and a flat and hydrophobic surface (PS) indicates the importance of the nanochannels in determining the capability of biomolecules adsorption. It is worth noting that in the case of our porous surface (curves a, a' of Figure 4) a deviation from the Langmuir fit is observed (curve a' of Figure 4) at higher concentration of protein in the initial solution.⁴³ This results can be rationalized considering that the Langmuir adsorption model fails significantly in many cases, especially when rough inhomogeneous surfaces, having multiple site-types available for adsorption, are present.⁴³

The Langmuir plot (that is C/Γ vs C) was extended also to the kinetic data of Mb adsorption onto the etched blend of Figure 3A obtained as a function of incubation time at 5 °C, for different Mb concentration (Figure 5 B). It is apparent that for incubation time less than 15 min no regular behavior is observed, probably because the equilibrium surface coverage is not reached. However, for incubation times higher than 15 min the adsorption kinetics can be described in terms of an equilibrium Langmuir behavior with parameters $K = 1$ and $\Gamma_m = 2.7$ due to the formation of a monolayer, regardless of incubation time and temperature (5 and 10 °C).

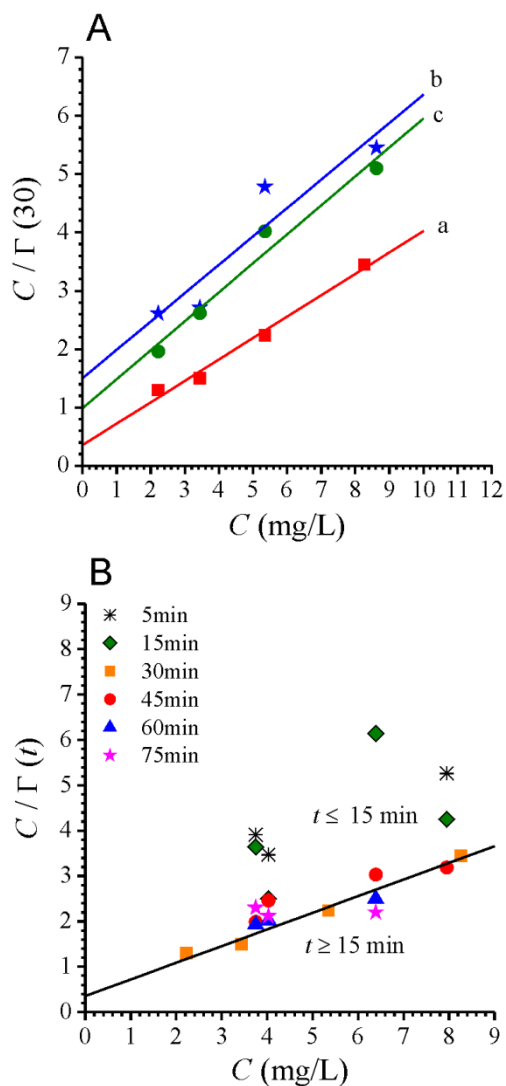


Figure 5. (A) Fit of Mb adsorption data of Figure 4 to the linear form of the Langmuir equation (Equation 3) in the case of the etched blend (curve a), PS thin film (curve b) and nude glass slide (curve c). The obtained values of Γ_m and K are reported in Table 1. Incubation was performed for 30 min, at 10°C. (B) Analysis of Mb adsorption data onto etched blend of Figure 3A for different incubation time (t), ranging from 5 to 75 min. The solid line corresponds to the Langmuir straight line equation (Equation 3) with $\Gamma_m = 2.7$ and $K = 1$. The data were obtained at 5 °C, except for the incubation time 30 min where a temperature of 10 °C was used.

We also studied the adsorption of Mb onto PS and our BCP-based thin films before and after removal of PLLA by means of neutron reflectometry (NR) measurements.³⁴ After measuring the reflectivity curves of the silicon support coated with the polymeric thin films in three different contrast liquids (Figure S5 and Table S1), D₂O solutions of Mb at concentration of 0.45 μM (7.9 mg/L) were deposited onto the supports. Reflectivity profiles were measured after 3 h of incubation time at 25°C. Since the protein was not deuterated, the sensitivity to adsorbed protein was enhanced by use of D₂O contrast. The comparison between the reflectivity profiles of the coated supports before and after Mb adsorption in D₂O contrast are reported in Figure 6, in the case of PS coating (Figure 6 A) and the PS-PLLA/PS-PEO coating before (Figure 6 B) and after (Figure 6 C, D) removal of PLLA. Reflectivity data measured using three different contrast were simultaneously fitted to a common model using the Aurore software application,⁴⁴ corresponding to the scattering density profiles (SLD) of Figure S5A',B' and to the red lines of Figure 6A and B. The resulting fitted parameters are instead reported in Table S1. As we already discussed in Ref. 23, modeling of the reflectometry data in the case of the etched blend (Figure 6 C, D) could not be accomplished with use of the standard box model approach, due to the intrinsic inhomogeneity of the nano-porous thin film.

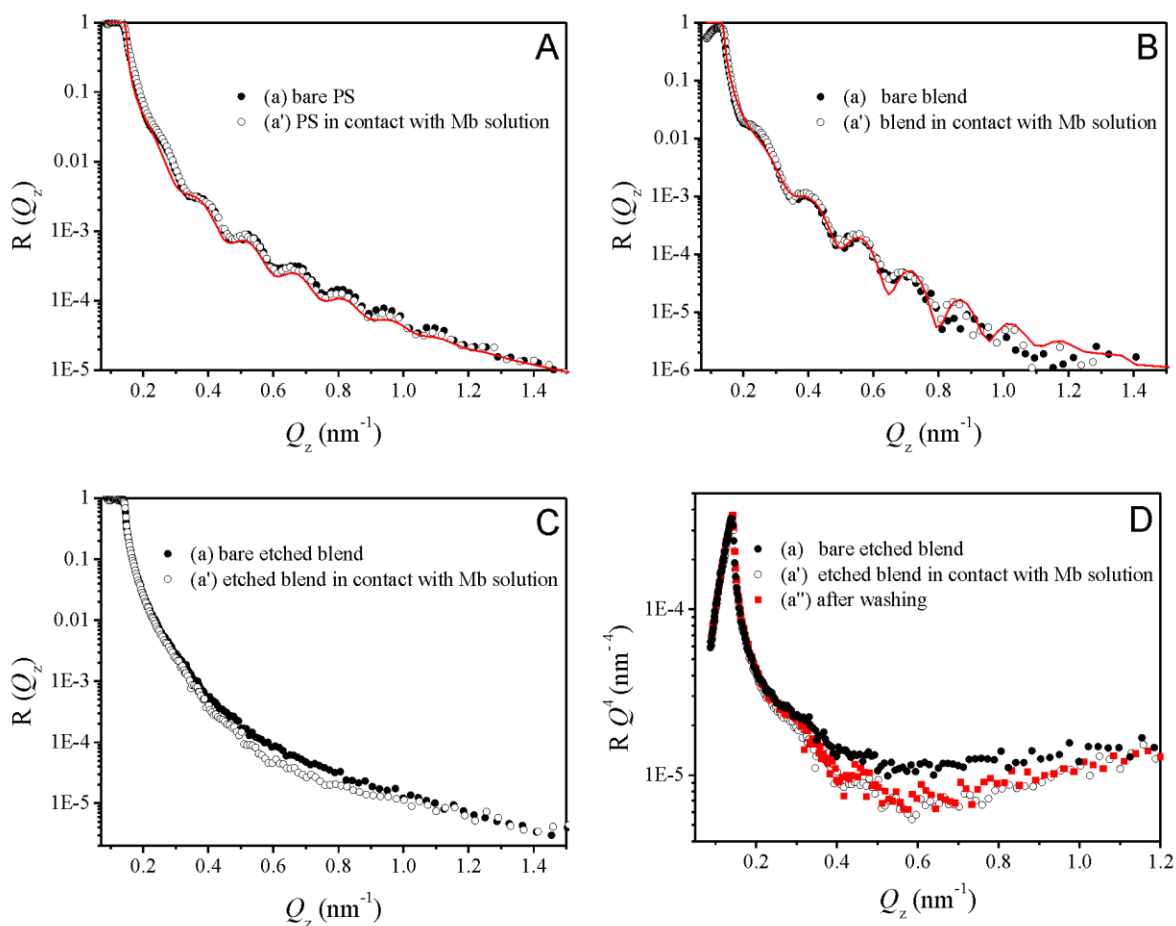


Figure 6. Experimental (symbols) and simulated (red lines) neutron reflectivity profiles as a function of the momentum transfer perpendicular to the surface Q_z of silicon supports coated with PS thin film (A) and PS-PLL/PS-PEO blend before (B) and after (C, D) removal of PLLA, acquired in presence of D_2O (\bullet , a) and in presence of D_2O containing Mb at a concentration of $0.45 \mu\text{M}$ (7.9 mg/L) after incubation for 3h (\circ , a'). In D, the reflectivity profiles (multiplied for Q^4 to enhance differences in the mid- and high- Q_z regions) of the etched blend in absence (\bullet , a) and in presence (\circ , a') of Mb are compared with the profile obtained in D_2O contrast after rinsing the support 3 times with 10 mL of H_2O (\blacksquare , a''). Error bars are not reported for clarity. Fits to the data are obtained according to the parameters listed in Table S1, and the neutron scattering length density profile (SLD) reported in Figure S5A' and B'.

The reflectivity profiles of PS (Figure 6 A) and non-etched blend (Figure 6 B) before (curves a) and after (curves a') the incubation with protein are almost identical, confirming little or no protein adsorption, in agreement with UV-Vis results. In the case of the BCP-based blend after PLLA removal (Figure 6 C), instead, a significant variation of the reflectivity profile is observed in presence of the solution containing Mb (compare curves a and a' of Figure 6 C). As shown in Figure 6 D, after multiplication of reflectivity by Q_z^4 , these differences are amplified (curves a and a' of Figure 6 D), especially in region $0.4 \text{ nm}^{-1} < Q_z < 0.8 \text{ nm}^{-1}$, confirming the non-negligible adsorption of Mb onto our BCP-based nanoporous support compared to PS and non-etched blend. Notably, the reflectivity profile of our porous blend containing adsorbed Mb after abundant rinsing (3 times with 10 mL of H₂O) remains identical to the profile acquired before rinsing (compare curves a' and a'' of Figure 6 D), demonstrating that quite strong interactions are established between the biomolecules and our porous surface by effect of simple physical adsorption.

Conclusions

Exploiting the partial miscibility of polyethylene oxide (PEO) and poly(L-lactide) (PLLA), and the possibility to easily remove PLLA blocks by basic hydrolysis, we set up a procedure that allows building nanostructured membranes with well-defined architecture containing pores ($\approx 20 \text{ nm}$ in width) delimited by PEO hydrophilic walls. The large surface area and the tailored pore sizes make the designed nanostructured material suitable support for the immobilization of specific biomolecules, compared with flat hydrophilic (glass) and hydrophobic non-porous (PS) surfaces. In particular, the study of adsorption of myoglobin onto the different supports with

different experimental techniques elucidates that our porous material exhibits an increased adsorption ability with respect to the other examined supports, indicating the importance of nanochannels in the process of adsorption of biomolecules. Results from this work provide a proof of the effect of different supports to protein adsorption and underline the importance to study adsorption behavior for individual systems of interest, since the extraction of general rules on adsorption phenomena when biological molecules are involved results quite difficult. It is worth noting that the designed procedure to prepare the BCP-based nanoporous material is general, robust, and versatile since it can be used to functionalize both solid (e.g. glass, silicon, gold) and flexible (e.g. polymeric membranes) supports. The functionalization of surfaces with our porous BCP-based material offers the possibility to tailor the properties of materials for biomedical and biotechnological applications, or for addressing specific usage conditions requiring controlled level of hydrophilicity/hydrophobicity, surface area, roughness, pore size and geometry and pore size distribution.

ASSOCIATED CONTENT

Supporting Information. The Supporting Information is available free of charge on the ACS Publications website. Additional experimental details (materials, thickness measurements, microscopy characterization, UV-Vis spectra, neutron reflectometry); Additional data (AFM characterization, additional data of Mb adsorption kinetics, TEM characterization on gold supports, quartz crystal microbalance (QCM) frequency vs time graphs, additional data of neutron reflectometry, table reporting the fitted parameters of the neutron reflectometry data) (PDF).

AUTHOR INFORMATION

Corresponding Author

*E-mail: anna.malafronte@unina.it ; *E-mail: finizia.auriemma@unina.it

Present Addresses

† School of Physical Sciences, University of Kent, Canterbury, Kent CT2 7NH, United Kingdom.

Notes

The authors declare no competing financial interest.

ACKNOWLEDGMENT

We thank Prof. Massimo Lazzari of the University of Santiago de Compostela (Spain) for collaboration in FESEM characterization and Prof. Angela Lombardi of the University of Naples (Italy) for her suggestions about performing of UV-Vis experiments and for useful discussions. The authors thank the Institut Laue-Langevin for the awarded beamtime and Dr. Philipp Gutfreund for the discussion about data analysis and reduction. This research was carried out in the frame of Programme STAR, financially supported by UniNA and Compagnia di San Paolo.

REFERENCES

- (1) Nakanishi, K.; Sakiyama, T.; Imamura, K. On the Adsorption of Proteins on Solid Surfaces, a Common but Very Complicated Phenomenon. *J. Biosci. Bioeng.* **2001**, *91*, 233-244.
- (2) Rabe, M.; Verdes, D.; Seeger, S. Understanding protein adsorption phenomena at solid surfaces. *Adv. Colloid Interface Sci.* **2011**, *162*, 87-106.
- (3) Norde, W. Adsorption of proteins at solid-liquid interfaces. *Cells and Materials* **1995**, *5*, 97-112.
- (4) Prieto-Simon, B.; Campas, M.; Marty, J.-L. Biomolecule Immobilization in Biosensor Development: Tailored Strategies Based on Affinity Interactions. *Protein Pept. Lett.* **2008**, *15*, 757-763.
- (5) Putzbach, W.; Ronkainen, N. J. Immobilization Techniques in the Fabrication of Nanomaterial-Based Electrochemical Biosensors: A Review. *Sensors* **2013**, *13*, 4811-4840.
- (6) Pinholt, C.; Hartvig, R. A.; Medlicott, N. J.; Jorgensen, L. The importance of interfaces in protein drug delivery - why is protein adsorption of interest in pharmaceutical formulations? *Expert Opin Drug Deliv.* **2011**, *8*, 949-964.
- (7) Zambrano, G.; Ruggiero E.; Malafronte, A.; Chino M.; Maglio, O.; Pavone, V.; Nastri, F.; Lombardi, A. Artificial heme enzymes for the construction of gold-based biomaterials. *Int. J. Mol. Sci.* **2018**, *19*, 2896.
- (8) Wilson, C. J.; Clegg, R. E.; Leavesley, D. I.; Percy, M. J. Mediation of biomaterial cell interactions by adsorbed proteins: a review. *Tissue Eng.* **2005**, *11*, 1-18.

- (9) Mitragotri, S.; Lahann, J. Physical approaches to biomaterial design. *Nature Mater.* **2009**, *8*, 15-23.
- (10) Cai, K.; Bossert, J.; Jandt, K. Does the nanometre scale topography of titanium influence protein adsorption and cell proliferation? *Colloid Surface B* **2006**, *49*, 136-144.
- (11) Han, M.; Sethuraman, A.; Kane, S. R.; Belfort, G. Nanometer-scale roughness having little effect on the amount or structure of adsorbed protein. *Langmuir* **2003**, *19*, 9868-9872.
- (12) Rechendorff, K.; Hovgaard, M. B.; Foss, M.; Zhdanov, V. P.; Besenbacher, F. Enhancement of protein adsorption induced by surface roughness. *Langmuir* **2006**, *22*, 10885-10888.
- (13) Riedel, M.; Muller, B.; Wintermantel, E. Protein adsorption and monocyte activation on germanium nanopyramids. *Biomaterials* **2001**, *22*, 2307-2316.
- (14) Ferreira, L.; Karp, J.; Nobre, L.; Langer, R. New opportunities: The use of nanotechnologies to manipulate and track stem cells. *Cell Stem Cell* **2008**, *3*, 136-146.
- (15) Goldberg, M.; Langer, R.; Jia, X. Nanostructured materials for applications in drug delivery and tissue engineering. *J Biomater. Sci. Polym. Ed.* **2007**, *18*, 241-268.
- (16) Liu, H.; Webster, T. Nanomedicine for implants: A review of studies and necessary experimental tools. *Biomaterials* **2007**, *28*, 354-369.
- (17) Nel, A.; Xia, T.; Mädler, L.; Li, N. Toxic Potential of Materials at the Nanolevel. *Science* **2006**, *311*, 622-627.

- (18) Patolsky, F.; Zheng, G.; Hayden, O.; Lakadamyali, M.; Zhuang, X.; Lieber, C. M. Electrical detection of single viruses. *Proc. Natl. Acad. Sci.* **2004**, *101*, 14017-14022.
- (19) Zheng, G.; Patolsky, F.; Cui, Y.; Wang, W. U.; Lieber, C. M. Multiplexed electrical detection of cancer markers with nanowire sensor arrays. *Nat. Biotechnol.* **2005**, *23*, 1294-1301.
- (20) Farokhzad, O. C.; Langer, R. Nanomedicine: Developing smarter therapeutic and diagnostic modalities. *Adv. Drug Deliv. Rev.* **2006**, *58*, 1456-1459.
- (21) Vamvakaki, V.; Chaniotakis, N. A. Immobilization of Enzymes into Nanocavities For the Improvement of Biosensor Stability. *Biosens. Bioelectron.* **2007**, *22*, 2650-2655.
- (22) Ravindra, R.; Zhao, S.; Gies, H.; Winter, R. Protein Encapsulation in Mesoporous Silicate: The Effects of Confinement on Protein Stability, Hydration, and Volumetric Properties. *J. Am. Chem. Soc.* **2004**, *126*, 12224-12225.
- (23) Auriemma, F.; De Rosa, C.; Malafronte, A.; Di Girolamo, R.; Santillo, C.; Gerelli, Y.; Fragneto, G.; Barker, R.; Pavone, V.; Maglio, O.; Lombardi, A. Nano-in-Nano Approach for Enzyme Immobilization Based on Block Copolymers. *ACS Appl. Mater. Interfaces* **2017**, *9*, 29318-29327.
- (24) Bates, F. S.; Fredrickson, G. H.. Block Copolymer Thermodynamics: Theory and Experiment. *Annu. Rev. Phys. Chem.* **1990**, *41*, 525-557.
- (25) Hamley, I. W. *The Physics of Block Copolymers*; Oxford University Press: Oxford, 1998.
- (26) Fasolka, M. J.; Mayes, A. M. Block Copolymer Thin Films: Physics and Applications. *Annu. Rev. Mater. Res.* **2001**, *31*, 323-355.

- (27) Hillmyer, M. A. Nanoporous Materials from Block Copolymer Precursors. *Adv. Polym. Sci.* **2005**, *190*, 137-181.
- (28) Mao, H.; Arrechea, P. L.; Bailey, T. S.; Johnsonw, B. J. S.; Hillmyer, M. A. Control of Pore Hydrophilicity in Ordered Nanoporous Polystyrene Using an AB/AC Block Copolymer Blending Strategy. *Faraday Discuss.* **2005**, *128*, 149-162.
- (29) Zalusky, A. S.; Olayo-Valles, R.; Wolf, J. H.; Hillmyer, M. A. Ordered Nanoporous Polymers from Polystyrene-Polylactide Block Copolymers. *J. Am. Chem. Soc.* **2002**, *124*, 12761-12763.
- (30) Olayo-Valles, R.; Lund, M. S.; Leighton, C.; Hillmyer, M. A. Large Area Nanolithographic Templates by Selective Etching of Chemically Stained Block Copolymer Thin Films. *J. Mater. Chem.* **2004**, *14*, 2729-273.
- (31) Antonini, E.; Brunori, M. *Hemoglobin and Myoglobin in Their Interactions with Ligands*; North Holland, Amsterdam, 1971.
- (32) Imai, K. *Metalloproteins, Chemical Properties, Biological Effects: Bioactive Molecules*; C. I. Otsuka and Y. Yamanaka eds, New York: Elsevier, 1988, p. 115.
- (33) Saerbeck, T.; Cubitt, R.; Wildes, A.; Manzin, G.; Andersen, K. H.; Gutfreund, P. Recent upgrades of the neutron reflectometer D17 at ILL. *J. Appl. Crystallogr.* **2018**, *51*, 249-256.
- (34) Malafronte, A.; Auriemma, F.; Barker, R.; Cioce, C.; Di Girolamo, R. Proposal 2015: Adsorption of undeuterated and deuterated myoglobin on a block copolymer surface with tailored nanopores size and hydrophilicity; Institut Laue-Langevin (ILL); doi:10.5291/ILL-DATA.9-13-608.

- (35) Penfold, J.; Thomas, R. K. The application of the specular reflection of neutrons to the study of surfaces and interfaces. *J. Phys.: Condens. Matter* **1990**, *2*, 1369-1412.
- (36) Cubitt, R.; G. Fragneto G. *Scattering in Microscopic Physics and Chemical Physics*; Academic Press, London, 2002.
- (37) Levantino, M.; Schirò, G.; Lemke, H. T.; Cottone, G.; Glowina, J. M.; Zhu, D.; Chollet, M.; Ihee, H.; Cupane, A.; Cammarata, M. Ultrafast myoglobin structural dynamics observed with an X-ray free-electron laser. *Nat. Commun.* **2015**, *6*, Article number: 6772.
- (38) Bergers, J. J.; Vingerhoeds, M. H.; van Bloois, L.; Herron, J. N.; Janssen, L. H. M.; Fischer, M. J. E.; Crommelin, D. J. A. The role of protein charge in protein-lipid interactions. pH-Dependent changes of the electrophoretic mobility of liposomes through adsorption of water-soluble, globular proteins. *Biochemistry* **1993**, *32*, 4641-4649.
- (39) Höök, F.; Vörös, J.; Rodahl, M.; Kurrat, R.; Böni, P.; Ramsden, J. J.; Textor, M.; Spencer, N.D.; Tengvall, P.; Gold, J.; Kasemo, B. A comparative study of protein adsorption on titanium oxide surfaces using in situ ellipsometry, optical waveguide lightmode spectroscopy, and quartz crystal microbalance/dissipation. *Colloids Surf. B* **2002**, *24*, 155-170.
- (40) Caruso, F.; Furlong, D. N.; Kingshott, P. Characterization of Ferritin Adsorption onto Gold. *J. Colloid Interface Sci.* **1997**, *187*, 129-140.
- (41) Muratsugu, M.; Ohta, F.; Miya, Y.; Hosokawa, T.; Kurosawa, S.; Kamo, N.; Ikeda, H. Quartz crystal microbalance for the detection of microgram quantities of human serum albumin: relationship between the frequency change and the mass of protein adsorbed. *Anal. Chem.* **1993**, *65*, 2933-2937.

(42) Norde, W. My voyage of discovery to proteins in flatland ...and beyond. *Colloids Surf. B* **2008**, *61*, 1-9.

(43) J. H. Kim, J. Y. Yoon. *Encyclopedia of Surface and Colloid Science*, **2002**, 4373.

(44) Gerelli, Y. Aurore: new software for neutron reflectivity data analysis. *J. Appl. Cryst.* **2016**, *49*, 330-339.

Table of Contents

